

Synthesis, Characterization, and Electrochemistry of Ruthenium Porphyrins Containing a Nitrosyl Axial Ligand

Karl M. Kadish,^{*,†} Victor A. Adamian,[†] Eric Van Caemelbecke,[†] Zheng Tan,[†] Pietro Tagliatesta,^{*,‡} Paola Bianco,[‡] Tristano Boschi,[‡] Geun-Bae Yi,[§] Masood A. Khan,[§] and George B. Richter-Addo^{*,§}

Department of Chemistry, University of Houston, Houston, Texas 77204-5641, Dipartimento di Scienze e Tecnologie Chimiche, Università di Roma Tor Vergata, Via della Ricerca Scientifica, 00133 Rome, Italy, and Department of Chemistry and Biochemistry, University of Oklahoma, 620 Parrington Oval, Norman, Oklahoma 73019

Received June 28, 1995[⊗]

Two ruthenium nitrosyl porphyrins have been synthesized and characterized by spectroscopic and electrochemical methods. The investigated compounds are represented as [(TPP)Ru(NO)(H₂O)]BF₄ and (TPP)Ru(NO)(ONO) where TPP is the dianion of 5,10,15,20-tetraphenylporphyrin. (TPP)Ru(NO)(ONO) crystallizes in the tetragonal space group *I*4, with *a* = 13.660(1) Å, *c* = 9.747(1) Å, *V* = 1818.7(3) Å³, and *Z* = 2, 233 K. The most chemically interesting feature of the structure is that the nitrosyl and O-bound nitrito groups are located axial and trans to one another. Both complexes undergo an irreversible reduction at the metal center which is accompanied by dissociation of the axial ligand trans to NO. The addition of 1–10 equiv of pyridine to [(TPP)Ru(NO)(H₂O)]BF₄ in CH₂Cl₂ containing 0.1 M TBAP leads to the formation of [(TPP)Ru(NO)(py)]⁺, a species which is reversibly reduced at *E*_{1/2} = −0.29 V. The electrochemical data indicate that (TPP)Ru(NO)(ONO) can also be converted to [(TPP)Ru(NO)(py)]⁺ in CH₂Cl₂ solutions containing pyridine but only under specific experimental conditions. This reaction does not involve a simple displacement of the ONO[−] axial ligand from (TPP)Ru(NO)(ONO) but occurs after reduction of (TPP)Ru(NO)(ONO) to (TPP)Ru(NO)(py) followed by reoxidation to [(TPP)Ru(NO)(py)]⁺.

Introduction

Nitrosyl–porphyrin complexes of iron have received a great deal of attention due to the important role that they play in biological systems.^{1–4} Mono-⁵ and bis(nitrosyl)⁶ complexes of iron porphyrins have been synthesized and characterized, and their electrochemistry has been explored in detail. However, much less attention has been given to the synthesis of the corresponding ruthenium nitrosyl porphyrins. There are three brief reports in the literature on ruthenium nitrosyl porphyrins. One involves a proposed bis-NO complex,⁷ while the others give brief mention of mononitrosyl halides^{8a} and methoxide.^{8b}

We now present our results on the synthesis, characterization, and electrochemistry of two ruthenium mononitrosyl porphyrins

of the form [(TPP)Ru(NO)(H₂O)]BF₄ and (TPP)Ru(NO)(ONO) where TPP represents the dianion of 5,10,15,20-tetraphenylporphyrin.

Experimental Section

Instrumentation and Procedure. NMR spectra were recorded on a Nicolet XL300 spectrometer. CDCl₃ was used as a solvent, and chemical shifts (δ , ppm) are referenced to internal TMS. FAB mass spectra were recorded on a VG-4 instrument using trinitro- or *m*-nitrobenzyl alcohol as matrix. Solution infrared spectra were measured by using a Bio-Rad FTS155 instrument or an IBM 32 FTIR spectrometer associated with an IBM 9000 computer system and an FTIR spectroelectrochemical cell whose design has been reported in the literature.⁹

Cyclic voltammetric measurements were performed using an EG&G Model 173 potentiostat in conjunction with a Princeton Applied Research Model RE0151 X-Y recorder. A three-electrode cell was utilized and consisted of a platinum working electrode, a platinum counter electrode, and a saturated calomel reference electrode (SCE). The reference electrode was separated from the bulk of the solution by a cracked-glass bridge filled with the appropriate solvent and supporting electrolyte. Deaeration of all solutions was accomplished by passing a stream of high purity nitrogen through the solution for 10 min prior to the measurements and then maintaining a blanket of nitrogen over the solution while making the measurements.

Chemicals. (TPP)Ru(CO) and NOBF₄ were purchased from Aldrich and used as received. All reactions were performed under an atmosphere of prepurified nitrogen. CH₂Cl₂ was distilled under nitrogen from CaH₂ while hexane and tetrahydrofuran (THF) were distilled under

[†] University of Houston.

[‡] Università di Roma Tor Vergata.

[§] University of Oklahoma.

[⊗] Abstract published in *Advance ACS Abstracts*, February 1, 1996.

- (1) (a) Stone, J. R.; Marletta, M. A. *Biochemistry* **1994**, *33*, 5636, and references therein. (b) Wang, J.; Rousseau, D. L.; Abu-Soud, H. M.; Stuehr, D. J. *Proc. Natl. Acad. Sci. U.S.A.* **1994**, *91*, 10512.
- (2) (a) Ignarro, L. J. *Semin. Hematol.* **1989**, *26*, 63. (b) Craven, P. A.; DeRubertis, F. R. *Biochim. Biophys. Acta* **1983**, *745*, 310. (c) Craven, P. A.; DeRubertis, F. R. *J. Biol. Chem.* **1978**, *253*, 8433.
- (3) (a) Yu, A. E.; Hu, S.; Spiro, T. G.; Burstyn, J. N. *J. Am. Chem. Soc.* **1994**, *116*, 4117. (b) Traylor, T. G.; Sharma, V. S. *Biochemistry* **1992**, *31*, 2847.
- (4) Selected reviews: (a) Moncada, S.; Palmer, R. M. J.; Higgs, E. A. *Pharmacol. Rev.* **1991**, *43*, 109. (b) Ignarro, L. J. *Annu. Rev. Pharmacol. Toxicol.* **1990**, *30*, 535.
- (5) (a) Scheidt, W. R.; Frisse, M. E. *J. Am. Chem. Soc.* **1975**, *97*, 17; (b) Mu, X. H.; Kadish, K. M. *Inorg. Chem.* **1988**, *27*, 4720; (c) Choi, I.-K.; Liu, Y.; Feng, D.; Paeng, K.-J.; Ryan, M. D. *Inorg. Chem.* **1991**, *30*, 1832; (d) Yoshimura, T. *Bull. Chem. Soc. Jpn.* **1991**, *64*, 2819; (e) Hoshino, M.; Ozawa, K.; Seki, H.; Ford, P. C. *J. Am. Chem. Soc.* **1993**, *115*, 9568.
- (6) (a) Lançon, D.; Kadish, K. M. *J. Am. Chem. Soc.* **1983**, *105*, 5610. (b) Wayland, B. B.; Olson, L. W. *J. Am. Chem. Soc.* **1974**, *96*, 6037.

(7) Srivastava, T. S.; Hoffman, L.; Tsutsui, M. *J. Am. Chem. Soc.* **1972**, *94*, 1385.

(8) (a) Massoudipour, M.; Pandey, K. K. *Inorg. Chim. Acta* **1989**, *160*, 115. (b) Antipas, A.; Buchler, J. W.; Gouterman, M.; Smith, P. D. *J. Am. Chem. Soc.*, **1978**, *100*, 3015.

(9) Lin, X. Q.; Mu, X. H.; Kadish, K. M. *Electroanalysis* **1989**, *1*, 35.

Table 1. Crystal Data and Structure Refinement for (TPP)Ru(NO)(ONO)

empirical formula (fw):	C ₄₄ H ₂₈ N ₆ O ₃ Ru (789.79)
temp =	213(2) K
λ =	0.710 73 Å
cryst syst:	tetragonal
space group:	<i>I</i> 4
Unit cell dimens	
<i>a</i> =	13.660(1) Å
<i>b</i> =	13.660(1) Å
<i>c</i> =	9.747(1) Å
<i>V</i> =	1818.7(3) Å ³
<i>Z</i> =	2
ρ (calcd) =	1.442 Mg/m ³
abs coeff:	0.481 mm ⁻¹
<i>F</i> (000) =	804
cryst size:	0.3 × 0.2 × 0.1 mm
θ range for data collection (deg):	2.11–25.00
index ranges:	0 < <i>h</i> < 16, 0 < <i>k</i> < 16, -11 < <i>l</i> < 2
no. of reflns colld:	1201
no. of indep reflns	1057 [<i>R</i> (int) = 0.0168]
refinement method:	full-matrix least-squares on <i>F</i> ²
data/restraints/params:	1055/0/138
goodness-of-fit on <i>F</i> ² :	0.967
final <i>R</i> indices (<i>I</i> > 2 σ (<i>I</i>)): ^{a,b}	<i>R</i> 1 = 0.0408, <i>wR</i> 2 = 0.1066
<i>R</i> indices (all data): ^{a,b}	<i>R</i> 1 = 0.0455, <i>wR</i> 2 = 0.1116
absolute struct param:	0.16(11)
largest diff peak and hole:	0.924 and -0.230 e Å ⁻³
^a <i>R</i> 1 = $\sum F_o - F_c / \sum F_o $. ^b <i>wR</i> 2 = $\{\sum [w(F_o^2 - F_c^2)^2] / \sum [wF_o^4]\}^{1/2}$.	

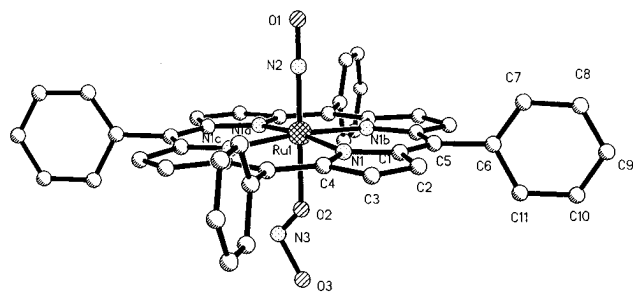
nitrogen from Na/benzophenone. Nitric oxide was purchased from Matheson and was purified by passage through KOH pellets and a cold trap (dry ice/acetone) to remove higher nitrogen oxides. Absolute CH₂-Cl₂ over molecular sieves (Fluka) and anhydrous pyridine (Aldrich) were used as received for electrochemistry. Tetra-*n*-butylammonium perchlorate, TBAP, purchased from Fluka, was recrystallized from absolute ethanol, and then dried and stored in a vacuum oven at 40 °C.

Synthesis of (TPP)Ru(NO)(ONO). Nitric oxide was bubbled for 10 min through a stirred CH₂Cl₂ (20 mL) solution of (TPP)Ru(CO) (0.100 g, 0.135 mmol) which was purged by argon before NO exposure. During this period, the color of the reaction solution changed from reddish-purple to dark red. The product was precipitated with hexane. The resulting solid was recrystallized from CH₂Cl₂/hexane (5:1) to give (TPP)Ru(NO)(ONO) (0.080 g, 0.104 mmol, 77% yield).

Anal. Calcd for C₄₄H₂₈O₃N₆Ru: C, 66.91; H, 3.57; N, 10.64; Found: C, 67.1; H, 3.6; N, 10.3. NMR (¹H, CDCl₃): 8.96 (s, 8H, pyrrole-H), 8.24 (d, *J* = 7 Hz, 4H, *o*-H of Ph), 8.15 (d, *J* = 9 Hz, 4H, *o*-H' of Ph), 7.75 (m, 12H, *m,p*-H of Ph). IR (KBr): ν_{NO} = 1852 cm⁻¹ (s), ν_{ONO} = 1520 and 932 cm⁻¹ (m). UV-vis (CH₂Cl₂): λ_{max} , nm (ϵ , mol⁻¹ L cm⁻¹) 410 (146 000), 558 (3000). Low resolution mass spectrum (FAB), *m/z* 744 [(TPP)Ru(NO)]⁺.

Synthesis of [(TPP)Ru(NO)(H₂O)]BF₄. To a CH₂Cl₂ solution (40 mL) of (TPP)Ru(CO) (0.200 g, 0.270 mmol) was added NOBF₄ (0.032 g, 0.270 mmol). The solution was stirred for 1 h during which the mixture turned dark red. Hexane (10 mL) was added to the reaction mixture, and the solvent was evaporated in air to give [(TPP)Ru(NO)(H₂O)]BF₄·0.2CH₂Cl₂ (0.173 g, 0.200 mmol, 74% yield). NMR (¹H, CDCl₃): 9.14 (s, 8H, pyrrole-H), 8.32 (m, 8H, *o*-H of Ph), 7.79 (m, 12H, *m,p*-H of Ph), 5.34 (s, 0.4H, CH₂Cl₂), -2.66 (2H, H₂O). IR (KBr): ν_{NO} = 1872 cm⁻¹ (s), ν_{BF_4} = 1054 cm⁻¹ (br). UV-vis (CH₂Cl₂): λ_{max} , nm (ϵ , mol⁻¹ L cm⁻¹) 404 (195 000), 558 (12 000). Anal. Calcd for C₄₄H₃₀O₂N₃BF₄Ru·0.2CH₂Cl₂: C, 61.33; H, 3.54; N, 8.09; Cl, 1.64. Found: C, 61.04; H, 3.87; N, 8.11; Cl, 1.66. Low resolution mass spectrum (FAB⁺): *m/z* 762 [(TPP)Ru(NO)(H₂O)]⁺ (6%), 744 [(TPP)Ru(NO)]⁺ (100%), 714 [(TPP)Ru]⁺ (46%).

Structural Determination of (TPP)Ru(NO)(ONO). A suitable crystal of (TPP)Ru(NO)(ONO) was grown by the slow evaporation of a CH₂Cl₂/hexane solution (5:1) at ambient temperature in air. Data were collected at -60(2) °C on a Siemens P4 diffractometer using monochromated MoK α radiation (λ = 0.710 73 Å) (Table 1). Data were corrected for Lorentz and polarization effects. No absorption

**Figure 1.** Molecular structure of (TPP)Ru(NO)(ONO). Hydrogen atoms have been omitted for clarity.

correction was applied since it was judged to be insignificant. The structure was solved using the *SHELXTL* (Siemens) system, and refined by full-matrix least-squares method on *F*² for all reflections (*SHELXL-93*).

Because of the pseudosymmetry and disorder of the structure, considerable difficulty was encountered during solution and refinement. A great deal of effort was made in correctly identifying the complex as (TPP)Ru(NO)(ONO). Initially, data were collected at room temperature, and the structure was solved and refined from those data. The data were re-collected at low temperature in an effort to improve its quality. Our attempts to collect the data below -60(2) °C were frustrated because the crystal undergoes what appears to be a reversible phase transition at -63 °C, and below that temperature all the peaks become broad or split into two peaks. Several data sets were collected between +22(2) and -60(2) °C. Solution and refinement were carried out for all of the data sets, and the best refinement was obtained from the -60 °C data set, for which results are presented here.

The data were consistent with three space groups, *I*4 (No. 79), $\bar{I}4$ (No. 82), and *I*4/*m* (No. 87). Although the intensity statistics suggested the noncentric space groups *I*4 or $\bar{I}4$, structure solution and refinement were tried for all three space groups. The best refinement was obtained in *I*4, which was selected as the correct choice.

The molecule is situated at the crystallographic four-fold center of symmetry, and only one-fourth is unique. The first difference map based on the Ru atom gave peaks for the complete porphyrin moiety and several peaks (2 eÅ⁻³ to 7 eÅ⁻³) along the axial direction. The second difference map based on the Ru atom, porphyrin moiety, and N2 and O1 atoms gave peaks for the O2, O3, and N3 atoms. Initially, we ignored the O3 peak and refined the structure with one linear and one bent NO ligand. However, the peak for O3 always appeared as a top peak in the difference map of 2.8 eÅ⁻³. It appears reasonable that the peaks in the difference map are more consistent with a model in which the axial positions are occupied with a linear NO and O-bonded ONO group. Subsequent refinement was based on that model. In the subsequent refinement cycles, NO and ONO atoms were refined anisotropically without any constraints, because a successful refinement of the thermal parameters (none of them became nonpositive definite or displayed unusual shapes (Figure 1)) of these atoms was considered a strong indication for the correctness of the chosen model. Other related models with ethoxide (which could in principle arise from a possible contaminant in the preparation of the starting (TPP)Ru(CO) using ethanol), or N-bound NO₂, instead of the O-bound ONO group were also tried, but were unstable and gave nonpositive definite thermal parameters. Also, the fact that the final difference map is featureless along the axial direction and the fact that the largest peak of 0.924 e Å⁻³ is situated 1.4 Å from the Ru atom in the porphyrin plane rule out the presence of an NO₃ group.

Given the limitations caused by the pseudosymmetry of the structure and the disorder of the ONO group, we feel that the choice of the (TPP)Ru(NO)(ONO) complex gives the best fit to the X-ray data. This conclusion is further supported by the analytical and spectroscopic data of crystals from the same batch. Despite all the difficulties stated above, the NO and ONO atomic positions were refined, and the refinement converged to give the final atomic positions in Figure 1 and Table 2. Nevertheless, accuracy of the bond lengths and angles involving the NO and ONO groups is severely compromised due to the factors stated above. Selected bond lengths and angles are collected in Table 3.

Table 2. Atomic coordinates ($\times 10^4$) and Equivalent Isotropic Displacement Parameters ($\text{\AA}^2 \times 10^3$) for (TPP)Ru(NO)(ONO)

atom	x	y	z	U_{eq}^a
Ru1	0	0	10000	33(1)
N1	-1446(3)	-391(3)	9875(14)	36(2)
C1	-1796(4)	-1335(5)	9846(15)	40(2)
C2	-2847(5)	-1297(5)	9803(15)	49(3)
C3	-3114(5)	-346(5)	9772(10)	42(2)
C4	-2229(4)	236(5)	9831(14)	41(2)
C5	-1249(5)	-2194(4)	9822(13)	40(2)
C6	-1795(5)	-3144(5)	9842(20)	48(3)
C9	-2831(6)	-4892(6)	9734(16)	61(5)
C7	-2088(14)	-3600(13)	10956(13)	78(4)
C8	-2624(15)	-4461(11)	10907(18)	88(5)
C10	-2531(10)	-4467(12)	8567(14)	66(4)
C11	-2011(10)	-3583(11)	8568(11)	56(3)
N2	0	0	11763(20)	38(4)
O1	0	0	12986(18)	62(6)
O3	0	0	6037(21)	125(9)
O2	0	0	7947(22)	73(7)
N3	263(34)	385(48)	7237(41)	79(23)

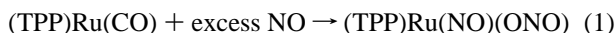
^a Equivalent isotropic U is defined as one-third of the trace of the orthogonalized U_{ij} tensor.

Table 3. Selected Bond Lengths (\AA) and Angles (deg) for (TPP)Ru(NO)(ONO)

Ru1-N2	1.72(2)	C1-C2	1.438(9)
Ru1-O2	2.00(2)	C2-C3	1.349(10)
Ru1-N1	2.050(5)	C3-C4	1.449(9)
N1-C4	1.370(8)	N2-O1	1.19(3)
N1-C1	1.376(8)	O3-N3	1.33(4)
C1-C5	1.391(9)	O2-N3	0.94(5)
N2-Ru1-O2	180.0	N1-C1-C2	108.3(6)
N2-Ru1-N1	93.4(4)	C5-C1-C2	124.5(6)
O2-Ru1-N1	86.6(4)	C3-C2-C1	107.8(6)
C4-N1-C1	108.3(5)	N1-C4-C3	108.0(6)
C4-N1-Ru1	126.2(4)	O1-N2-Ru1	180.0
C1-N1-Ru1	125.5(4)	N3-O2-Ru1	137(3)
N1-C1-C5	127.2(6)	O2-N3-O3	109(5)

Results and Discussion

Reaction of the five-coordinate (TPP)Ru(CO) carbonyl compound with excess NO gas results in the displacement of the CO ligand and generation of the six-coordinate nitrosyl nitrito derivative in 77% isolated yield (eq 1). The (TPP)Ru(NO)(ONO) compound is air-stable in the solid state and is

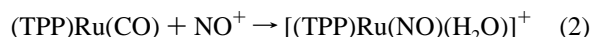


soluble in common polar organic solvents. This product has been characterized by elemental analysis and conventional spectroscopic techniques. In particular, its IR spectrum as a KBr pellet reveals the presence of a band at 1852 cm^{-1} attributed to the linear NO ligand. This value for ν_{NO} is slightly lower than those reported for the halide complexes (TPP)Ru(NO)X ($X = \text{Cl}^-$ (1880 cm^{-1}) or Br^- (1884 cm^{-1})).^{8a} Two medium intensity bands at 1520 and 932 cm^{-1} are attributed to the coordinated nitrito group.¹⁰ Interestingly, the 1520 cm^{-1} band of the ONO group also lies in the acceptable range for bent NO ligands.¹¹ In order to resolve any ambiguity in the identity of the product of eq 1, we subjected a suitable crystal to an X-ray crystallographic analysis. The molecular structure of the complex is shown in Figure 1. Selected bond distances and angles are collected in Table 3. The most chemically interesting

feature about the structure is that the Ru atom sits in the plane of the porphyrin nitrogens, and the NO and ONO ligands are trans to one another. The NO ligand is linear, and this feature is consistent with the nitrosyl nitrito product being a $\{\text{Ru}(\text{NO})\}^6$ complex using the Enemark-Feltham notation.¹² Only one-fourth of the molecule is crystallographically unique, and the N3 atom of the O-bound nitrite is disordered over four positions. To our knowledge, this is the first crystallographically characterized Ru nitrosyl porphyrin, and is the first structurally characterized six-coordinate complex of the type (P)M(NO)(X) where P is a porphyrin macrocycle and X an anionic ligand.

The formation of (TPP)Ru(NO)(ONO) from (TPP)Ru(CO) and NO gas is not unusual.¹¹ Wilkinson has synthesized Ru(sal₂en)(NO)(ONO) (sal₂en = *N,N'*-ethylenebis(salicylideneoimino)) from Ru(sal₂en)(PPh₃)₂ and nitric oxide in THF.¹³ To the best of our knowledge, Ru(sal₂en)(NO)(ONO) is the only other structurally characterized metal complex containing a trans arrangement of nitrosyl and nitrito groups. Indeed, the Ru-N(nitrosyl) and Ru-O(nitrito) distances in Ru(sal₂en)(NO)(ONO) of 1.713 and 2.011 \AA compare favorably with those of (TPP)Ru(NO)(ONO) (1.72(2) and 2.00(2) \AA , respectively). Yoshimura has also observed the formation of (P)Fe(NO)(NO₂) (P = TPP or protoporphyrin IX dimethylester) when solutions of the five-coordinate (P)Fe(NO) are exposed to excess NO gas.^{14,15} Lukehart also reported the synthesis of [Cr(NO)(ONO)₂(pyridine)₃](pyridine) from the reaction of Cr(CO)₆ with NO in THF followed by addition of pyridine.¹⁶

The air-stable cationic mononitrosyl complex [(TPP)Ru(NO)(H₂O)]BF₄ is prepared by a simple substitution of the CO ligand in (TPP)Ru(CO) with the nitrosonium cation (eq 2).¹⁷ The IR



spectrum of this aqua complex reveals a band at 1872 cm^{-1} that is assigned to ν_{NO} . It also shows a band at 1054 cm^{-1} due to uncoordinated tetrafluoroborate anion.

Despite attempts to generate (TPP)Ru(NO)₂, no evidence of this species could be obtained although its formation cannot be ruled out as an intermediate in eq 1. Interestingly, the low resolution mass spectra of the ruthenium nitrosyl porphyrins indicate that the Ru-NO bonds in these complexes remain intact during mass spectral measurements. This is unusual, given the tendency of nitrosyl metalloporphyrins to lose their NO ligands readily under mass spectral measurement conditions, and suggests a strong Ru-NO bond.

Electroreduction of [(TPP)Ru(NO)(H₂O)]⁺. A cyclic voltammogram of [(TPP)Ru(NO)(H₂O)]⁺ in CH₂Cl₂ containing 0.1 M TBAP is shown in Figure 2a. The compound undergoes reductions at $E_{\text{pc}} = -0.33$ and $E_{\text{pc}} = -0.78$ V and at $E_{1/2} = -1.05$ V. The cyclic voltammogram suggests an equilibrium between two forms of the initial compound in solution and this is also suggested by the IR data. The spectrum of [(TPP)Ru(NO)(H₂O)]BF₄ in neat CH₂Cl₂ is characterized by a ν_{NO} of 1882 cm^{-1} but there are overlapping IR bands at 1880 and 1870 cm^{-1} in CH₂Cl₂ solutions containing 0.1 M TBAP. These bands

(12) Feltham, R. D.; Enemark, J. H. *Top. Stereochem.* **1981**, *12*, 155.

(13) Carrondo, M. A. A. F. C. T.; Rudolf, P. R.; Skapski, A. C.; Thornback, J. R.; Wilkinson, G. *Inorg. Chim. Acta* **1977**, *24*, L95.

(14) Yoshimura, T. *Inorg. Chim. Acta* **1984**, *83*, 17.

(15) A related anionic [(TPP)Fe(NO)(ONO)]⁻ has been proposed to form when (TPP)FeX ($X = \text{anionic ligand}$) is reacted with excess nitrite ion: Finnegan, M. G.; Lappin, A. G.; Scheidt, W. R. *Inorg. Chem.* **1990**, *29*, 181.

(16) Lukehart, C. M.; Troup, J. M. *Inorg. Chim. Acta* **1977**, *22*, 81.

(17) The crystal structure of a related [(OEP)Ru(NO)(H₂O)]⁺ derivative has been determined: Yi, G.-B.; Khan, M. A.; Richter-Addo, G. B. Submitted for publication.

(10) (a) Nakamoto, K. *Infrared and Raman Spectra of Inorganic and Coordination Compounds*, 4th ed.; Wiley-Interscience: New York, 1986; p 224. (b) Hitchman, M. A.; Rowbottom, G. L. *Coord. Chem. Rev.* **1982**, *42*, 55.

(11) Richter-Addo, G. B.; Legzdins, P. *Metal Nitrosyls*; Oxford University Press: New York, 1992; Chapter 2.

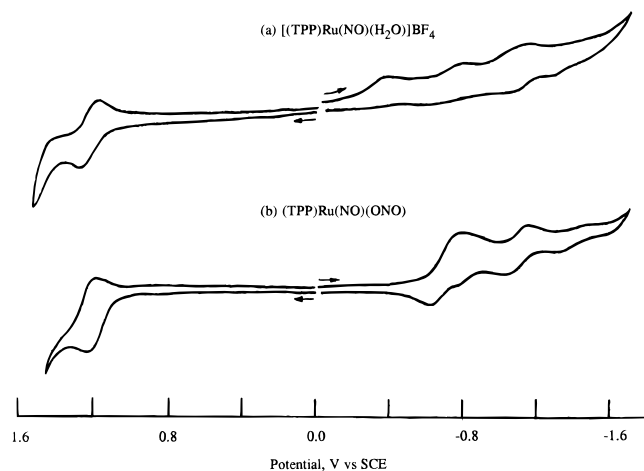
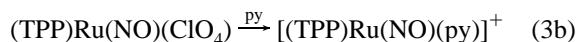
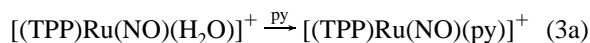


Figure 2. Cyclic voltammograms of (a) $[(\text{TPP})\text{Ru}(\text{NO})(\text{H}_2\text{O})]\text{BF}_4$ and (b) $(\text{TPP})\text{Ru}(\text{NO})(\text{ONO})$ in CH_2Cl_2 , containing 0.1 M TBAP. Scan rate = 0.1 V/s.

are of the same intensity, consistent with the presence of two different axially coordinated ligands trans to the NO. One would be H_2O (in the original compound) and the other could be ClO_4^- from the supporting electrolyte. However, as will be shown below, the addition of pyridine to $[(\text{TPP})\text{Ru}(\text{NO})(\text{H}_2\text{O})]^+$ in CH_2Cl_2 leads to a single redox couple at $E_{1/2} = -0.29$ V and the presence of only one IR band at 1879 cm^{-1} .

The first reduction of $[(\text{TPP})\text{Ru}(\text{NO})(\text{H}_2\text{O})]^+$ remains irreversible in CH_2Cl_2 at scan rates up to 5 V/s or at temperatures as low as $-50\text{ }^\circ\text{C}$. However, this process becomes reversible and occurs at $E_{1/2} = -0.29$ V upon addition of 1–10 equiv of pyridine to the CH_2Cl_2 solution. At the same time, the second reduction peak at $E_{\text{pc}} = -0.78$ V disappears and the current for the first increases in magnitude, consistent with the presence of a single species in solution. This transition from an irreversible to a reversible process is illustrated by the voltammograms in Figure 3a. The data suggest that a pyridine molecule replaces the axial ligand trans to NO in both species present in solution thus giving $[(\text{TPP})\text{Ru}(\text{NO})(\text{py})]^+$ as shown by eq 3.



There is no evidence for the conversion of $[(\text{TPP})\text{Ru}(\text{NO})(\text{H}_2\text{O})]^+$ to $[(\text{TPP})\text{Ru}^{\text{III}}(\text{py})_2]^+$ in the absence of an applied potential. The electrochemistry of $(\text{TPP})\text{Ru}^{\text{II}}(\text{py})_2$ and $[(\text{TPP})\text{Ru}^{\text{III}}(\text{py})_2]^+$ is well-known and characterized by a $\text{Ru}(\text{II})/\text{Ru}(\text{III})$ process at $\approx +0.21$ V in CH_2Cl_2 .¹⁸ Cyclic voltammograms of $[(\text{TPP})\text{Ru}(\text{NO})(\text{H}_2\text{O})]^+$ show no such process at potentials close to $+0.21$ V. In addition, a strong NO band is seen at 1879 cm^{-1} in CH_2Cl_2 /pyridine mixtures, and this further confirms that NO is still coordinated under these solution conditions.

On the other hand, the NO axial ligand can be displaced by a second pyridine molecule on the slower time scales of thin-layer cyclic voltammetry or differential pulse voltammetry under the application of a positive potential. Under these experimental conditions, the equilibrium in eq 4 is shifted toward the right due to the more facile reduction of $[(\text{TPP})\text{Ru}^{\text{III}}(\text{py})_2]^+$ ($E_{1/2} = +0.21$ V) as compared to $[(\text{TPP})\text{Ru}(\text{NO})(\text{py})]^+$ ($E_{1/2} = -0.29$

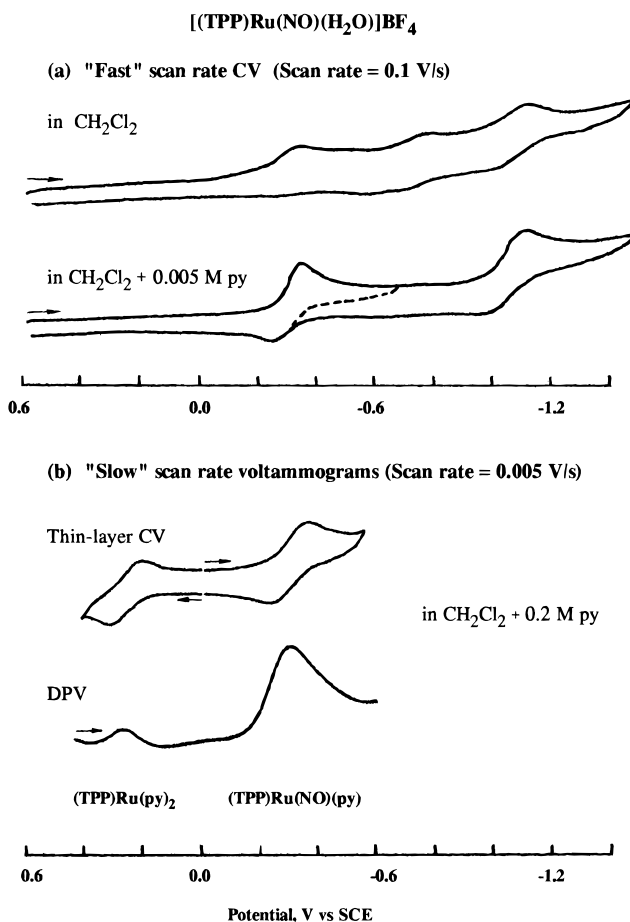
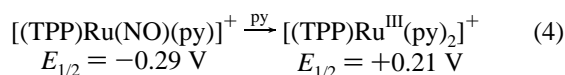


Figure 3. (a) Conventional cyclic voltammograms (scan rate = 0.1 V/s) of $[(\text{TPP})\text{Ru}(\text{NO})(\text{H}_2\text{O})]\text{BF}_4$ in CH_2Cl_2 containing 0.1 M TBAP before and after addition of 5×10^{-3} M py and (b) slow scan rate (0.005 V/s) thin-layer cyclic and differential pulse voltammograms of the same compound in CH_2Cl_2 containing 0.2 M pyridine and 0.2 M TBAP.

V) and this leads to formation of the bis-pyridine $\text{Ru}(\text{III})$ adduct which is reversibly reduced to $(\text{TPP})\text{Ru}^{\text{II}}(\text{py})_2$.



The electrochemically induced formation of the bis(pyridine)- $\text{Ru}(\text{III})$ derivative is illustrated in Figure 3b which shows thin-layer and differential pulse voltammograms of $[(\text{TPP})\text{Ru}(\text{NO})(\text{H}_2\text{O})]^+$ in CH_2Cl_2 containing 0.2 M pyridine. Both voltammograms exhibit peaks due to the $[(\text{TPP})\text{Ru}(\text{py})_2]^+ / (\text{TPP})\text{Ru}(\text{py})_2$ redox couple ($E_{1/2} = +0.21$ V) despite the fact that virtually none of this compound is initially present in the bulk of solution.

Electroreduction of $(\text{TPP})\text{Ru}(\text{NO})(\text{ONO})$. A conventional cyclic voltammogram (scan rate = 0.1 V/s) of $(\text{TPP})\text{Ru}(\text{NO})(\text{ONO})$ in CH_2Cl_2 , 0.1 M TBAP is shown in Figure 2b. Under these conditions, the compound undergoes three reductions. The first is a broad irreversible one-electron process at $E_{\text{pc}} \approx -0.8$ V which is coupled with two reoxidation peaks at $E_{\text{pa}} \approx -0.76$ and -0.56 V. Two additional reductions occur at $E_{1/2} = -1.06$ and $E_{\text{pc}} \approx -1.46$ V, and both have peak currents significantly lower than the peak current of the first reduction. Overall, the cyclic voltammogram in Figure 2b suggests that the first reduction of $(\text{TPP})\text{Ru}(\text{NO})(\text{ONO})$ is followed by a chemical reaction, the products of which are reduced at $E_{\text{pc}} = -1.16$ and $E_{\text{pc}} \approx -1.46$ V or oxidized at $E_{\text{pa}} = -0.76$ and -0.56 V.

(18) Brown, G. M.; Hopf, F. R.; Ferguson, J. A.; Meyer, T. J.; Whitten, D. G. *J. Am. Chem. Soc.* **1973**, *95*, 5939.

Scheme 1

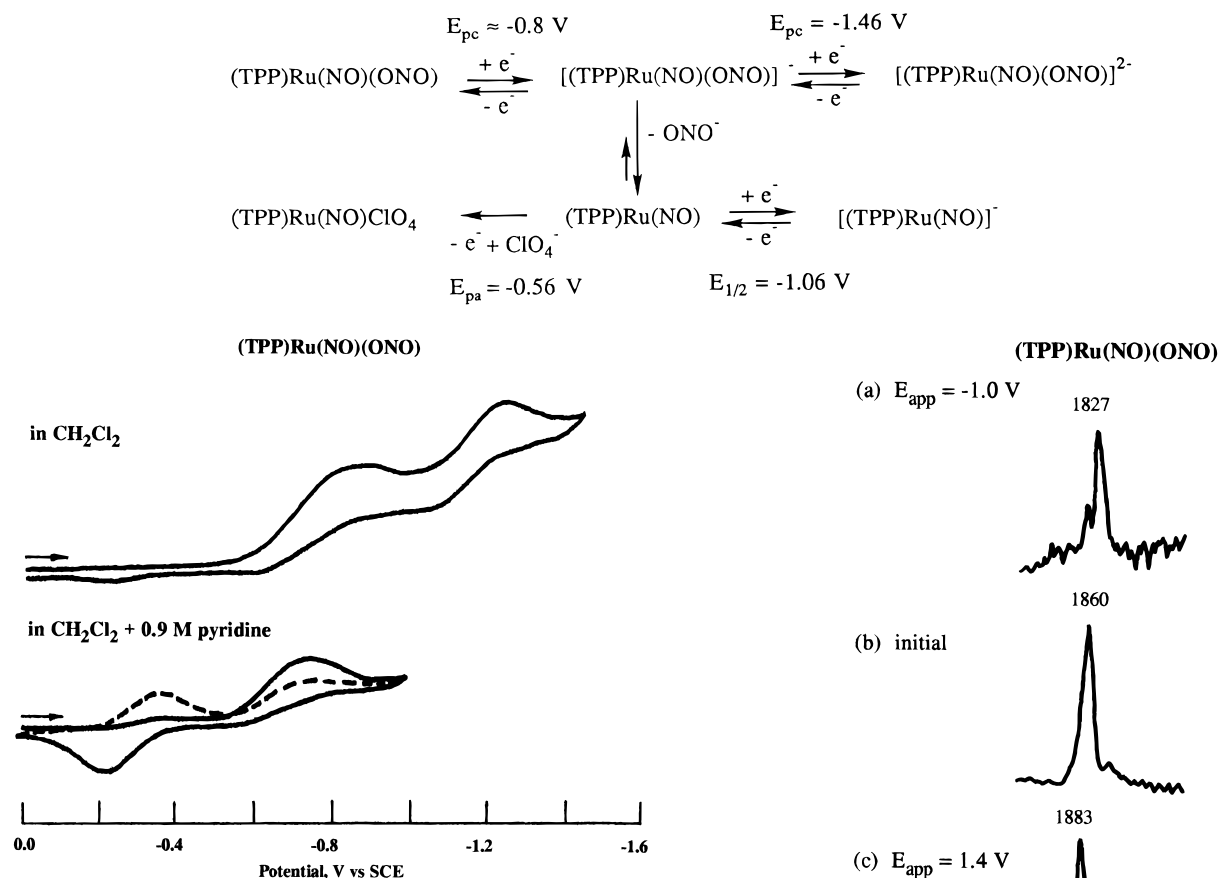


Figure 4. Thin-layer cyclic voltammograms of (TPP)Ru(NO)(ONO) obtained in CH₂Cl₂ containing 0.2 M TBAP with and without 0.9 M pyridine for one (—) and two (---) scans. Scan rate = 0.005 V/s.

A slow scan rate (0.005 V/s) thin-layer cyclic voltammogram of (TPP)Ru(NO)(ONO) in CH₂Cl₂ is shown in Figure 4. In this case, only two reductions (at $E_{pc} \approx -0.8$ and $E_{1/2} = -1.06$ V) of equal height are seen. The IR spectrum obtained after controlled-potential reduction of (TPP)Ru(NO)(ONO) at -1.0 V in CH₂Cl₂ containing 0.1 M TBAP is shown in Figure 5a. The singly reduced product is characterized by an NO band at 1827 cm^{-1} as compared to the initial NO band which is located at 1860 cm^{-1} (Figure 5b).¹⁹ Thus, the thin-layer IR spectroelectrochemical data suggest that the NO axial ligand remains coordinated upon controlled potential reduction by one electron and it also indicates the presence of only one nitrosyl product on the time scale of the spectroelectrochemical experiment.

Overall, the electrochemical and spectroelectrochemical data suggest that the reduced species, $[(\text{TPP)Ru(NO)(ONO)}]^-$, is slowly converted to (TPP)Ru(NO) due to dissociation of the ONO⁻ axial ligand. The formation of two reduced species, i.e., $[(\text{TPP)Ru(NO)(ONO)}]^-$ and (TPP)Ru(NO), is observed by

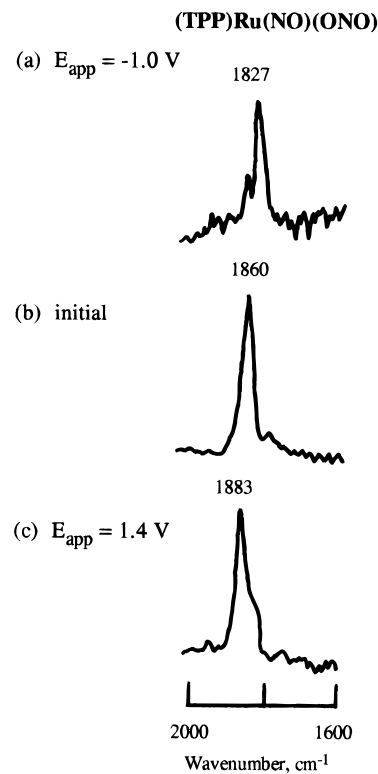


Figure 5. IR absorption spectra showing the NO vibration of (TPP)Ru(NO)(ONO) in its (a) singly reduced, (b) neutral, and (c) singly oxidized forms in CH₂Cl₂ containing 0.2 M TBAP.

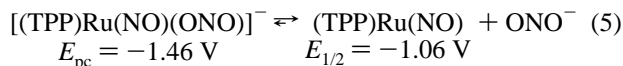
conventional cyclic voltammetry (Figure 2b), but only one, (TPP)Ru(NO), is observed using the "slow-scan" techniques of FTIR thin-layer spectroelectrochemistry and thin-layer cyclic voltammetry. The presence of two reduction products on the conventional cyclic voltammetric time scale can explain the two reoxidation peaks at -0.56 and -0.76 V. The anodic peak at -0.76 V is proposed to involve a reoxidation of electrogenerated $[(\text{TPP)Ru(NO)(ONO)}]^-$ to (TPP)Ru(NO)(ONO) while the peak at -0.56 V is proposed to involve an oxidation of the intermediate (TPP)Ru(NO) to (TPP)Ru(NO)ClO₄. The overall set of redox processes observed during reduction of (TPP)Ru(NO)(ONO) in CH₂Cl₂ is then proposed to occur as shown in Scheme 1.

The formation of a proposed (TPP)Ru(NO) product on the thin-layer time scale and $[(\text{TPP)Ru(NO)(ONO)}]^-$ on the more rapid cyclic voltammetric time scale is also consistent with the occurrence of two reduction processes following the initial one-electron transfer at ~ -0.8 V (Figure 2b). The binding of the anionic ONO⁻ group in (TPP)Ru(NO)(ONO) leads to a more difficult reduction and, as is the case for most metalloporphyrins, the potential is shifted by 300 mV or more for each added anionic axial ligand.²⁰ The separation between the reductions at $E_{1/2} = -1.06$ V ($E_{pc} = -1.15$ V) and $E_{pc} = -1.46$ V is

(19) (a) Chemical reduction of (i) $[(\text{TPP)Ru(NO)(H}_2\text{O)}]^+$ with cobaltocene or (ii) (TPP)Ru(NO)(ONO) with sodium borohydride also results in generation of a complex with ν_{NO} at 1824 cm^{-1} . The same product may also be obtained from reaction of (TPP)Ru(CO) with a minimum amount of NO gas. We believe that all three experiments lead to an identical porphyrin product in solution, i.e., (TPP)Ru(NO), the same as generated upon electrochemical reduction of $[(\text{TPP)Ru(NO)(H}_2\text{O)}]^+$ or (TPP)Ru(NO)(ONO). We have isolated the chemically reduced species, and further characterization of the product is in progress. It is possible that, during isolation, the suggested (TPP)Ru(NO) species is converted to (TPP)Ru(NO)(L) which has a similar ν_{NO} .^{19b} (b) During revision of this manuscript, we learned of the preparation and structural characterization of related (porphyrin)Ru(NO)(OH) compounds with nitrosyl stretches around 1820 cm^{-1} : Ford, P. C.; Miranda, K. Private communication.

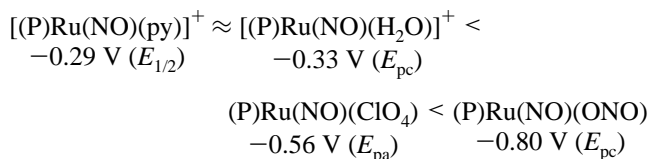
therefore consistent with the process at $E_{1/2} = -1.06$ V being assigned as a reduction of the intermediate (TPP)Ru(NO) and the one at -1.46 V to the reduction of [(TPP)Ru(NO)(ONO)]⁻.

It should be noted however, that the presence of a "(TPP)Ru(NO)" process in Figure 2b does not mean that a high concentration of this species may actually be in solution.²⁰ This is because the 310 mV separation between the two redox reactions would be a driving force that could lead to an electrochemically induced dissociation of the ONO⁻ axial ligand from the more difficult to reduce [(TPP)Ru(NO)(ONO)]⁻ species prior to electroreduction *via* the five-coordinate species, i.e. an electrochemical CE mechanism. In fact, in the extreme, the solution could contain only [(TPP)Ru(NO)(ONO)]⁻ but still be reduced completely *via* the more thermodynamically favorable process involving the putative (TPP)Ru(NO).



Additional evidence for the equilibrium shown in eq 5 is given by the following two observations: (i) the sum of the currents for the second and third reductions of (TPP)Ru(NO)(ONO) are about equal to those for the first reduction under routine cyclic voltammetric conditions (see Figure 2b) and (ii) only two reductions (at $E_{\text{pc}} \approx -0.8$ and $E_{1/2} = -1.06$ V) of equal peak height are seen on the thin-layer cyclic voltammograms of (TPP)Ru(NO)(ONO) (see Figure 4). This is consistent with a shift of eq 5 completely towards the right under conditions of thin-layer cyclic voltammetry.

The peak and/or half-wave potentials for reduction of the [(TPP)Ru(NO)(L)]⁺ complexes (L = py, H₂O, ONO⁻ or ClO₄⁻) follow the overall charge of the compound and the nature of the counterion:

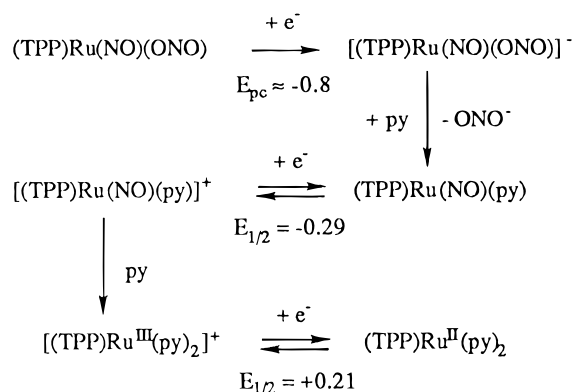


The electrochemical data indicate that (TPP)Ru(NO)(ONO) can also be converted to [(TPP)Ru(NO)(py)]⁺ in CH₂Cl₂ solutions containing pyridine but only under specific experimental conditions. This reaction does not involve a simple displacement of the ONO⁻ axial ligand from (TPP)Ru(NO)(ONO) but occurs after reduction of (TPP)Ru(NO)(ONO) to (TPP)Ru(NO)(py) followed by reoxidation to [(TPP)Ru(NO)(py)]⁺. This is illustrated by the thin-layer cyclic voltammograms in Figure 4. [(TPP)Ru(NO)(py)]⁺ is not initially present in the solution containing pyridine (as shown by the lack of a well-defined reversible reaction at $E_{1/2} = -0.29$ V) but this species is electrogenerated after reversibly sweeping the potential between 0.0 and -1.0 V.

The data in Figures 3 and 4 are thus self-consistent and, in the case of (TPP)Ru(NO)(ONO) in CH₂Cl₂/py mixtures, suggest the electron transfers and coupled chemical reactions given in Scheme 2.

The key point in Scheme 2 is that the three Ru complexes on the left can be seen on slow time scales and all three undergo formal reduction processes, with the exact potential depending

Scheme 2



upon the specific set of axial ligands. Thus, the neutral "nitrosyl-nitrito" compound is irreversibly reduced at ≈ -0.80 V, the cationic "nitrosyl-pyridine" compound is reversibly reduced at -0.29 V, and the cationic "bis(pyridine)" compound is reversibly reduced at $+0.21$ V.

Electrooxidation. As seen in Figure 2, [(TPP)Ru(NO)(H₂O)]⁺ and (TPP)Ru(NO)(ONO) both appear to undergo similar reversible oxidations in CH₂Cl₂ containing 0.1 M TBAP. However, a close examination of the voltammograms shows this not to be the case. [(TPP)Ru(NO)(H₂O)]⁺ indeed undergoes a reversible to quasireversible one-electron transfer with $E_{1/2} = 1.26$ V and a peak-to-peak separation of 80 mV. However, (TPP)Ru(NO)(ONO) has $E_{\text{pa}} = 1.23$ V and $E_{\text{pc}} = 1.21$ V, and this 20 mV peak-to-peak separation is inconsistent with the theoretically expected 60 mV separation between E_{pc} and E_{pa} for a reversible one-electron transfer. Such a small value of ΔE_{p} can only be accounted for by a multielectron transfer (which does not occur), by adsorption (which does not occur), or by the occurrence of two separate redox couples. In the latter case one must invoke a chemical reaction following oxidation, the most likely of which would be a replacement of ONO⁻ by ClO₄⁻ from the supporting electrolyte (which is present in 0.1 M concentration). This would lead to [(TPP)Ru(NO)ClO₄]⁺ as the first oxidation product of (TPP)Ru(NO)(ONO), thus giving (TPP)Ru(NO)ClO₄ upon rereduction at $E_{\text{pc}} = 1.21$ V. A monitoring of the IR spectrum during thin-layer controlled potential oxidation of (TPP)Ru(NO)(ONO) shows the disappearance of the initial band at 1860 cm⁻¹ and the appearance of a band at 1883 cm⁻¹ (Figure 5c). On the basis of the electrochemistry of (TPP)Ru(NO)(ONO), this latter band is assigned to [(TPP)Ru(NO)ClO₄]⁺.

Acknowledgment. Financial support for this work was provided by (i) the Robert A. Welch Foundation (K.M.K., Grant E-680), (ii) by MURST and the CNR (P.T.), and (iii) by startup funds of the University of Oklahoma (G.B.R.-A.). We are also grateful to Professor P. C. Ford for providing us information on his work with (porphyrin)Ru(NO)X (X = ONO, OH) prior to publication. We also wish to thank Drs. Francesca Polizio, Baoheng Han, and Francis D'Souza for helpful discussions and Dr. Ning Guo and Ms. Tianshu Ma for several IR measurements.

Supporting Information Available: Computer drawings showing 4-fold disorder of N3 of the ONO group and a thermal ellipsoid diagram, tables of crystal data, anisotropic displacement parameters, hydrogen coordinates, and isotropic displacement parameters of (TPP)Ru(NO)(ONO), and text describing SHELX93 (11 pages). Ordering information is given on any current masthead page.